Post-Limit Deformation Behaviour of Materials and the Analysis of Zonal Disintegration of Rocks around Underground Excavations

Chanyshev, A.I. and Belousova, O.E.

***Abstract*—Based on the analysis of the post-limit deformation stage, it is shown that under soft loading of rocks, displacement rate greatly increases in the post-limit deformation zone, and the kinetic energy grows as well. It is supposed that given the kinetic energy reaches a certain threshold value, a rock block exposed to the post-limit deformation splits off the rock mass. This assumption is applied to studying the phenomenon of zonal disintegration of rocks surrounding deep cylindrical tunnels.**

***Index Terms*—Kinetic energy, post-limit deformation, zonal disintegration**

I. Introduction

It is conventional that rock mass around deep excavations is zoned as follows: a destruction zone immediately adjoins an excavation, and then there is a plastic strain zone followed with an elastic strain zone. The destruction zone is the poorest studied. The priority questions on how does rock mass fail and what are the laws of this failure remain unanswered. Destruction around deep excavations shows itself first of all as the oriented fracturing. The same pattern can been seen when breaking window glass with a hard object: a web of fractures appears, some fractures delineate the hole contour, other make net of radial fractures. There are several zones of oriented fractures around deep tunnels, these zones are spaced as a rule at $\sqrt{2}\,a$, where a is the tunnel radius, or the average radius of "false" contour [Oparin, 2008; Shemyakin, 1992; Shemyakin, 1986; Kurlenya, 1996].

Destruction of a material is described using equations that characterize behaviour of the material during failure. For example, the deformable solid mechanics introduces the concept of post-limit deformation of rocks. This is a branch of the "shear stress—displacement curve", that is obtained under loading samples by stiff presses, under pre-set displacements of the loader grips in time t. The load is corrected every time it is applied (modern presses are equipped with servo-valves to implement the loading adjustment). Figure 1 shows a typical curve of the shear stress and displacement [Goodman, 1987]: loading is applied up to the point A, whereupon post-limit deformation takes place.

Chanyshev, A.I., Dr. Phys.-Math., Head, Rock Failure Laboratory, N.A. Chinakal Institute of Mining, Siberian Branch, Russian Academy of Sciences, 54 Krasny Prospect, 630091 Novosibirsk, Russia (phone: +7 383-335-97-50, e-mail: belousova_o@ngs.ru)

Belousova, O.E. PhD Eng, N.A. Chinakal Institute of Mining, Siberian Branch, Russian Academy of Sciences, 54 Krasny Prospect, 630091 Novosibirsk, Russia, (phone: +7 383-335-97-50, e-mail: belousova_o@ngs.ru)

II. Equations of the Material Behaviour

It is worth pointing out that if the load τ is fixed and retained constant for a long time at the point C of the curve in Fig. 1, the material will "creep", the displacement will grow from γ_C to γ_D, and later on the material will go to the descending branch ADB of the curve $\tau = \tau(\gamma)$ [Goodman, 1987]. If the said is included in plotting the curve $\gamma = \gamma(t)$, the result will be the deformation pattern shown in Fig. 2.

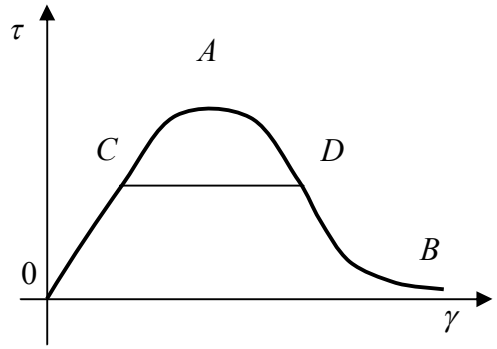

Fig.1. Typical curve of creep in medium under deformation.

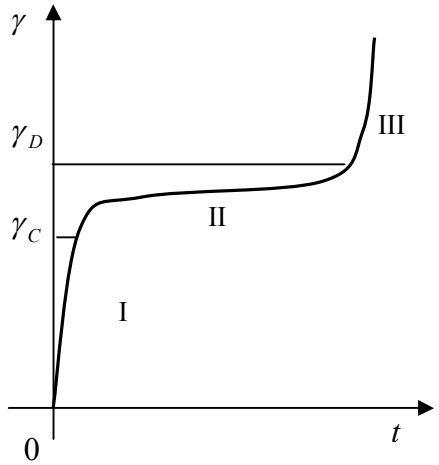

Fig. 2. Typical shear stress τ and displacement curve from [Goodman, 1987].

The curve in Fig. 2 consists of: branch I—elastic loading of material up to the point *C* in Fig. 1; branch II—the transfer from *C* to the point *D* (Fig. 1); branch III—the post-

ISBN: 978-988-19252-2-0
ISSN: 2078-0958 (Print); ISSN: 2078-0966 (Online)

limit deformation branch ADB of the curve $\tau = \tau(\gamma)$ in Fig. 1. Kovrizhnykh [Kovrizhnykh, 2008] introduced the term "perfect creep" to describe the branch III in Fig. 2, on the analogy with the perfect plasticity. He suggested that the stress τ_∞, correspondent to long-term strength, holds constant afterwards. This is a debatable assertion, since, as seen in Fig. 1, the stress τ drops as it goes to the branch ADB and induces growth of the strain γ, that is, the stress is not constant. Thus, it is necessary to include the post-limit deformation branch in Fig. 1 in analyzing, for instance, zonal disintegration of rocks around deep excavations and in other analyses.

To begin with, the "stress—strain" curve illustrates material resistance to deformation. Let the value of a load F exerted on a material change with increasing t. Let the material resistance be R. These values are related under the Newton law:

$$m\,\ddot{x} = F - R$$

It follows from Fig. 1 that R can differ from F. When F exceeds R, which is especially pronounced at the post-limit deformation stage, accelerations arise and kinetic energy grows. On an assumption that the kinetic energy reached in a fractured zone in rocks increases fast up to a critical value as compared with the neighbouring zones, the fractured rock zone can lose contact with the rock mass (the kinetic energy is converted to the potential energy of fracture). The fracturing de-stresses the rock mass. The de-stressing on the plane of break results in loading of the rest rock mass. The process of the zonal disintegration in rocks continues.

Mathematical modeling of the post-limit deformation involves the notion of the proper tensor basis. We take the experiment of the pre-limit and post-limit deformation of quartzite samples [Bieniawsky, 1983]. Figure 3 shows the curves $\sigma_Z = \sigma_Z(\varepsilon_Z)$, $\sigma_Z = \sigma_Z(\varepsilon_\varphi)$ obtained in uniaxial compression of a cylindrical quartzite sample. The stress and strain tensors are, respectively:

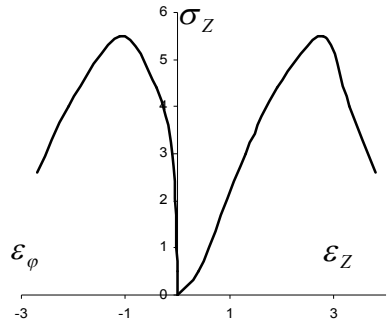

Fig. 3. $\sigma_Z = \sigma_Z(\varepsilon_Z)$ and $\sigma_Z = \sigma_Z(\varepsilon_\varphi)$ in quartzite under uniaxial compression.

$$T_\sigma = \begin{pmatrix} \sigma_Z & 0 & 0 \\ 0 & 0 & 0 \\ 0 & 0 & 0 \end{pmatrix},\ T_\varepsilon = \begin{pmatrix} \varepsilon_Z & 0 & 0 \\ 0 & \varepsilon_\varphi & 0 \\ 0 & 0 & \varepsilon_r \end{pmatrix}.$$

Here, $\varepsilon_\varphi = \varepsilon_r$ due to that r, φ are perpendicular to z and the material is assumed initially isotropic. To describe the tensors above, we introduce identity tensors:

$$T_1 = \frac{1}{\sqrt{3}}\begin{pmatrix} 1 & 0 & 0 \\ 0 & 1 & 0 \\ 0 & 0 & 1 \end{pmatrix},\ T_2 = \frac{1}{\sqrt{6}}\begin{pmatrix} 2 & 0 & 0 \\ 0 & -1 & 0 \\ 0 & 0 & -1 \end{pmatrix},$$

$$T_3 = \frac{1}{\sqrt{2}}\begin{pmatrix} 0 & 0 & 0 \\ 0 & 1 & 0 \\ 0 & 0 & -1 \end{pmatrix}.$$

Projections of T_σ, T_ε on unitary vectors are denoted as S_1, S_2, S_3, Ω_1, Ω_2, Ω_3, respectively. Evidently, $S_3 = \Omega_3 \equiv 0$. The relations $S_1 = S_1(\Omega_1)$, $S_2 = S_2(\Omega_2)$ for quartzite are shown in Fig. 4.

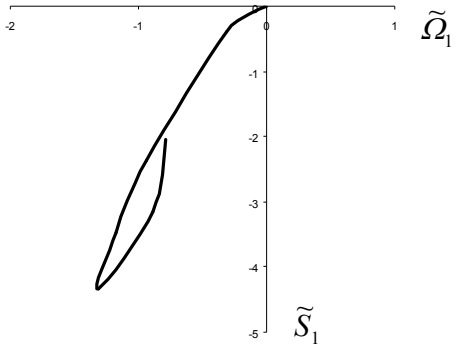

Fig. 4a. The curves of $\widetilde{\Omega}_2$ plotted based on [Bieniawsky, 1983]: $\widetilde{S}_1$, $\widetilde{\Omega}_1$ coincide with average stress and strain accurate to numerical

Revolve the basis T_1, T_2 clockwise, and the curve in Fig. 4a will flatten while the curve in Fig. 4b will descend (the revolved basis coordinates are S_1, $\Im_1$, S_2, $\Im_2$). At a certain moment (when $\varphi = \varphi_*$) the curve in Fig. 4 will become nearly straight line. In quartzite the angle $\varphi_* = 16.6^\circ$. Figure 5 shows $\widetilde{S}_1$, $\widetilde{\Im}_1$, $\widetilde{S}_2$, $\widetilde{\Im}_2$ in the tensor basis revolved at $\varphi_* = 16.6^\circ$; here:

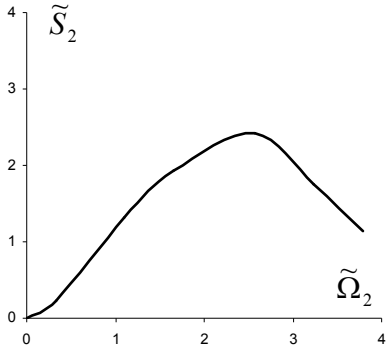

Fig. 4b. The curves of $\widetilde{S}_2 = \widetilde{S}_2(\widetilde{\Omega}_2)$ plotted based on [Bieniawsky, 1983]: $\widetilde{S}_2$, $\widetilde{\Omega}_2$ coincide with shear stress intensity and shear strain.

$$\widetilde{S}_1 = S_1 \cos\varphi_* - S_2 \sin\varphi_*,$$
$$\widetilde{S}_2 = S_2 \sin\varphi_* + S_2 \cos\varphi_*,$$
$$\widetilde{\Im}_1 = \Im_1 \cos\varphi_* - \Im_2 \sin\varphi_*,$$
$$\widetilde{\Im}_2 = \Im_2 \sin\varphi_* + \Im_2 \cos\varphi_*.$$

The papers [Chanyshev, 2002; Chanyshev, 2003] showed

ISBN: 978-988-19252-2-0
ISSN: 2078-0958 (Print); ISSN: 2078-0966 (Online)

that the curves $\widetilde{S}_2 = \widetilde{S}_2(\widetilde{\Im}_2)$ are universal for any type of loading; i.e., these curves are the rated relationships for an initially isotropic material. Any material has its angle φ_*, straight line with the slope α and the curve $\widetilde{S}_2 = \widetilde{S}_2(\widetilde{\Im}_2)$.

The calculations of the zonal disintegration phenomenon assume that $\widetilde{S}_1 = \widetilde{\Im}_1/\lambda_1$ (Fig. 5a), where λ_1 is constant

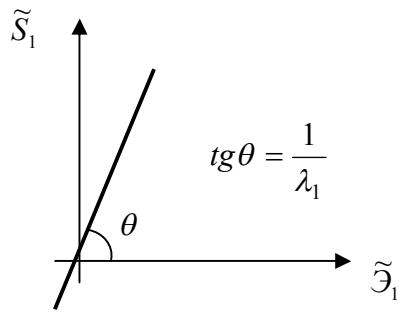

Fig. 5a. Proportional curve of the stress $\widetilde{S}_1$ versus strain $\widetilde{\Im}_1$.

under any state of a medium. To simplify the calculations, it is suggested to use the curve $\widetilde{S}_2 = \widetilde{S}_2(\widetilde{\Im}_2)$ in Fig. 5b, including plasticity and post-limit deformation. Thus, we have derived an analog of the deformation plasticity theory.

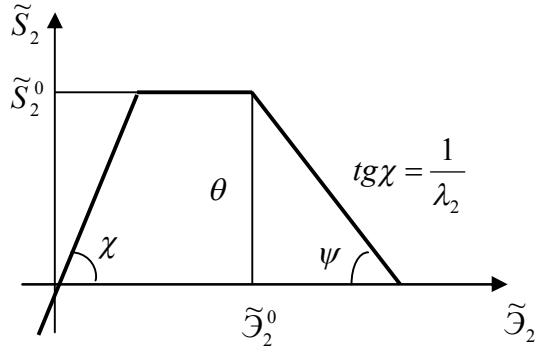

Fig. 5b. The change of the "shear" stress $\widetilde{S}_2$ versus "shear" $\widetilde{\Im}_2$: the elastic, plastic and post-limit deformation stages.

III. Mathematical Modeling

Let a rock mass with an excavation having radius $r = a$ be in the plain strain state. There are two dimensions available: a—the excavation radius and b—the external radius. The boundary conditions at the radial contours are:

$$\sigma_r\big|_{r=a} = 0,\ \sigma_r\big|_{r=b} = -p(t),\ \ p(t) = p_1 \cdot t,\ p(t) \geq 0 \quad (1)$$

and the initial conditions are:

$$u\big|_{t=0} = 0,\quad \left.\frac{\partial u}{\partial t}\right|_{t=0} = 0. \quad (2)$$

The problem solution requires relating the stresses σ_r, σ_θ and strains ε_r, ε_θ. Considering that:

$$\widetilde{\Im}_1 = \varepsilon_r \cos\alpha + \varepsilon_\theta \sin\alpha,$$
$$\widetilde{\Im}_2 = -\varepsilon_r \sin\alpha + \varepsilon_\theta \cos\alpha,$$
$$\widetilde{S}_1 = \sigma_r \cos\alpha + \sigma_\theta \sin\alpha$$
$$\widetilde{S}_2 = -\sigma_r \sin\alpha + \sigma_\theta \cos\alpha$$

from (2), derive the elastic relations in the form:

$$\begin{cases} \varepsilon_r = a_{11}\sigma_r - a_{12}\sigma_\theta, \\ \varepsilon_\theta = -a_{12}\sigma_r + a_{22}\sigma_\theta, \end{cases}$$

where

$$\begin{cases} a_{11} = \lambda_1 \cos^2\alpha + \lambda_2 \sin^2\alpha, \\ a_{22} = \lambda_1 \sin^2\alpha + \lambda_2 \cos^2\alpha, \\ a_{12} = (\lambda_2 - \lambda_1)\sin\alpha\cos\alpha. \end{cases} \quad (3)$$

The post-limit deformation relations are obtained in the same form:

$$\begin{cases} \varepsilon_r \cos\alpha + \varepsilon_\theta \sin\alpha = \lambda_1(\sigma_r \cos\alpha + \sigma_\theta \sin\alpha), \\ \varepsilon_r \sin\alpha - \varepsilon_\theta \cos\alpha - \widetilde{\Im}_2^0 = \lambda_2^*(\widetilde{S}_2^0 - \widetilde{S}_2), \end{cases} \quad (4)$$

where $\widetilde{\Im}_2^0$, $\widetilde{S}_2^0$—respectively, the peak-strength strains and stresses in the curve $\widetilde{S}_2 = \widetilde{S}_2(\widetilde{\Im}_2)$; $1/\lambda_*$—the drop modulus of this curve; the angle $\alpha = \varphi_* + \pi/4$.

It is worthy to notice that the flexibilities a_{22} and a_{11} differ in (3), which means that $a_{22} - a_{11} = (\lambda_2 - \lambda_1)\cos 2\alpha$, or that material is anisotropic. In case when $\lambda_2 - \lambda_1 \succ 0$, a_{22} is higher than a_{11}. On the other hand, if $\alpha \neq \pi/4$, dilatancy takes place: $\alpha \succ \pi/4$ expands the volume of a medium since the shear stress is positive $(\sigma_r - \sigma_\theta)/2$ and the material is loosened; when $0 \prec \alpha \prec \pi/4$, the volume of the medium diminishes, the material is compacted.

The calculations are limited to an "incompressible" material ($\lambda_1 = 0$) and two branches of the deformation curve $\widetilde{S}_2 = \widetilde{S}_2(\widetilde{\Im}_2)$, namely, the elasticity and post-limit deformation. Taking into account that $\lambda_1 = 0$, we have:

$$\varepsilon_r \cos\alpha + \varepsilon_\theta \sin\alpha = 0. \quad (5)$$

Since $\varepsilon_r = \partial u/\partial r$, $\varepsilon_\theta = u/r$, then:

$$u = \frac{A(t)}{r^{tg\alpha}}. \quad (6)$$

Substituting (6) in (4) and then in the equilibrium equation:

$$\frac{\partial \sigma_r}{\partial r} + \frac{\sigma_r - \sigma_\theta}{r} = \rho \frac{\partial^2 u}{\partial t^2}, \quad (7)$$

yields a formula of σ_r in terms on an arbitrary function $A(t)$ and an arbitrary constant.

The same procedure with the equilibrium equation at the post-limit deformation stage allows an identical formula to find σ_r in the post-limit deformation zone.

Application of the boundary conditions (1), the conditions for continuity of the stresses σ_r, σ_θ and displacement u

ISBN: 978-988-19252-2-0
ISSN: 2078-0958 (Print); ISSN: 2078-0966 (Online)

at the interface between the elasticity and post-limit deformation zones, and the introduced denotation:

$$A(t) = -\lambda_2 \widetilde{S}_2^0 X(t)\cos\alpha \cdot a^{tg\alpha+1}, \qquad (8)$$

will result in an equation to find $X = X(t)$:

$$\Lambda^2 \ddot{X} = X\frac{\cos\alpha}{\sin 2\alpha}\left\{\left(\frac{a}{b}\right)^{2tg(\alpha)} + \frac{\lambda_2}{\lambda_2^*}\right\} -$$
$$- X^{-\frac{tg(\alpha)-1}{tg(\alpha)+1}}\left\{\frac{\cos\alpha}{\sin 2\alpha} + \left(1+\frac{\lambda_2}{\lambda_2^*}\right)\frac{1}{\cos\alpha}\frac{1}{(1-tg\alpha)}\right\} -$$
$$- \frac{\lambda_2}{\lambda_2^*}\frac{\cos\alpha}{\sin 2\alpha} X^{-\frac{2tg\alpha}{tg\alpha+1}} + \frac{p(t)}{\widetilde{S}_2^0}\left(\frac{a}{b}\right)^{tg\alpha-1} +$$
$$+ \frac{1}{\cos\alpha}\left(1+\frac{\lambda_2}{\lambda_2^*}\right)\frac{1}{1-tg\alpha}, \qquad (9)$$

where

$$\Lambda = \sqrt{\frac{2(1-tg\alpha)}{\rho\lambda_2\cos\alpha a^2\left[\left(\frac{a}{b}\right)^{2(tg\alpha-1)} - 1\right]}}.$$

By definition, $\mathrm{X}(t) = c^2/a^2$, where $r = c$ coincides with the interface between the elasticity and destruction zones ($r = a$—the initial excavation radius). This is the second order equation for determining $\mathrm{X} = \mathrm{X}(t)$, and it requires setting the initial conditions $\mathrm{X}(t_0), \dot{\mathrm{X}}(t_0)$ from the elastic problem solution. The radial stresses in the elastic zone are:

$$\sigma_r^y = -\frac{\mathrm{X}(t)\cos\alpha\widetilde{S}_2^0}{\sin 2\alpha}\left(\left(\frac{r}{b}\right)^{tg\alpha-1} - \left(\frac{b}{r}\right)^{tg\alpha+1}\right)\times$$
$$\times\left(\frac{a}{b}\right)^{tg\alpha+1} - p(t)\left(\frac{r}{b}\right)^{tg\alpha-1} -$$
$$- \frac{\rho\ddot{\mathrm{X}}(t)\lambda_2\widetilde{S}_2^0\cos\alpha\ ab}{2(1-tg\alpha)}\left(\frac{a}{b}\right)^{tg\alpha}\times\left(\left(\frac{b}{r}\right)^{tg\alpha-1} - \left(\frac{r}{b}\right)^{tg\alpha-1}\right). \qquad (10)$$

The radial stresses in the destruction zone are:

$$\sigma_r^p = \frac{\widetilde{S}_2^0}{\cos\alpha}\left(1+\frac{\lambda_2}{\lambda_2^*}\right)\frac{1}{1-tg\alpha}\left[\left(\frac{a}{r}\right)^{1-tg\alpha} - 1\right] -$$
$$- \frac{\rho\lambda_2\widetilde{S}_2^0 a^2}{2(1-tg\alpha)}\left[\left(\frac{r}{a}\right)^{1-tg\alpha} - \left(\frac{a}{r}\right)^{1-tg\alpha}\right]\ddot{X}(t) -$$
$$- \frac{\lambda_2}{\lambda_2^*}\frac{\widetilde{S}_2^0\cos\alpha}{\sin 2\alpha}\left[\left(\frac{a}{r}\right)^{1+tg\alpha} - \left(\frac{a}{r}\right)^{1-tg\alpha}\right]X(t). \qquad (11)$$

The shear stresses in the elasticity and destruction zones are:

$$\sigma_\theta^y = \sigma_r^y tg\alpha + \frac{1}{\lambda_2}\left(\frac{u}{r} - tg\alpha\frac{\partial u}{\partial r}\right),$$
$$\sigma_\theta^p = \sigma_r^r tg\alpha + \lambda_2\widetilde{S}_2^0 X\frac{a^{tg\alpha+1}}{r^{tg\alpha+1}\lambda_2^*\cos\alpha}. \qquad (12)$$

The formulas (10)—(12) are valid given the following conditions hold true: (A) boundary conditions (8) are satisfied at the boundaries $r = a$ and $r = b$; (B) the conditions of continuity:

$$\sigma_r^y\Big|_{r=c} = \sigma_r^p\Big|_{r=c}, \qquad u^y\Big|_{r=c} = u^p\Big|_{r=c},$$

are fulfilled at the elasticity and destruction zones interface $r = c$; and (C) the kinetic energy is below its critical value in the destruction zone. After the third condition has been violated, the destruction zone starts splitting off the rock mass. The reached value of $\sigma_r^y\Big|_{r=c}$ will drop to zero according to a certain law, and de-stressing of the rest rock mass (elasticity zone) will imply the rock mass loading and another destruction zone origination. The calculation formulas also include corrective terms associated with the time-dependent boundary conditions at the "false" contour $r = c$, which are withdrawn from the present paper due to awkwardness.

The calculations comprised the following parameters: $\lambda_1 = 0$, internal radius $a = 1$ m, external radius $b = 9$ m, radius-wise step 0.1. Table 1 describes mechanical properties of tested rocks.

TABLE 1
MECHANICAL PROPERTIES OF ROCKS.

Rock	$\lambda_2 = 10^{-11}$, Pa^{-1}	$\lambda_2^* = 10^{-11}$, Pa^{-1}	S_2^0, MPa	ρ, kg/m^3
Marble	3,7	2,9	42	2700
Diabase	2,2	3,7	120	2900
Sandstone	4,9	1,6	46	2700

The calculations were accomplished as follows. First, we solved the pure elastic problem. Under the pre-set boundary conditions (8), we estimated stresses, strains and displacements at $r = a$, and the displacement rate as the member of the initial conditions for the derivative $\mathrm{X}(t)$ at the time $t = t_0$ when the contour $r = a$ transfers to the destruction stage. Then, using the Runge—Kutta method, we solved the dynamic equation for determining $\mathrm{X} = \mathrm{X}(t)$ at any other time. The formulas (6)—(12) allowed finding displacements, displacement rates, strains and stresses. Later on, we calculated kinetic energy in the destruction zone. When the radius c equaled $\sqrt{2}a$, we recorded the value of the kinetic energy T and the related time t_*. From this moment, the value of σ_r at the false contour $r = c$ started downward to zero. The calculations assumed the linear decrease of σ_r. The loading drop rate was varied in the calculations. After the destruction zone had split off the rock mass, it was withdrawn from the analysis, and the elastic deformation zone was only studied. When loading dropped to zero at $r = c$, a "new" destruction zone began originating in the "old" elastic strain zone. The dynamic equation for $\mathrm{X} = \mathrm{X}(t)$ was solved again under the other initial and boundary conditions, and the kinetic energy was again calculated. The critical value of the kinetic energy, related to the destruction zone size, was used for determining a new zone-to-zone interface that, broadly speaking, may differ from the product of $\sqrt{2}$ and the previous radius of excavation. In addition, we determined conditions for the

ISBN: 978-988-19252-2-0
ISSN: 2078-0958 (Print); ISSN: 2078-0966 (Online)

loading rate to be such that geometric sequence of the boundaries between the zones of disintegration has denominator $\sqrt{2}$; analyzed the influence of the de-stressing rate and the elastic modulus to drop modulus ratio, and the value of the angle α on the process of the zonal disintegration. The calculation results are presented below.

Figure 6a shows the split-off energy density versus the

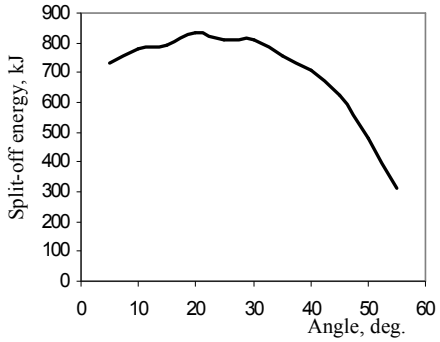

Fig. 6a. The split-off energy density against the angle α in marble.

angle α for marble. At $\alpha = 20^\circ \div 30^\circ$ the energy density is maximum and the material is compacted under shears. When α is above 60°, loosening takes place in the material and the contour of excavations is continuously being crushed. Total loading time (to the formation of ruptured zone 3) is $T \approx 10^{-3}$ s. Maximum pressure at the external contour is $p \approx 2.5 S_2^0$.

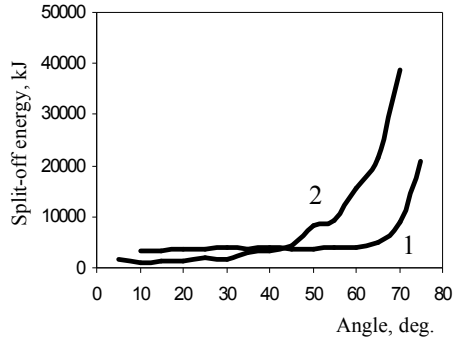

Fig. 6b. The split-off energy density against the angle α : 1—sandstone: 2—diabase.

On the fig. 6b dependence of the energy necessary for splitting off from the angle α for sandstone and diabase is presented. At the values of the angle α smaller than 60° slow growth of energy is observed.

If the values of the angle α are bigger than 60° then exponential energy growth takes place.

On the fig. 7 dependence of density of the energy, necessary for splitting off, on speed of stress for sandstone, diabase and marble is shown. On external border of the calculated medium loading changed from $1{,}05\widetilde{S}_2^0$ to $5\widetilde{S}_2^0$.

Other calculations are devoted to research of influence of parameters of stressing (loading rate at $r = b$, elastic modulus/drop modulus ratio, de-stressing rate at $r = c$) on the formation of disintegration zones with radii to be within the geometric progression with denominator $\sqrt{2}$.

Based on the analysis of the data, the following conclusions have been drawn:

- the slow loading induces continuous crushing and fragmentation of rocks;
- under loading at rates higher than $V = 40$ MPa/s, the disintegration zones are formed according to geometric progression by distance of the zone from the excavation center, with denominator $\sqrt{2}$;
- the rate of de-stressing and the ratio of the elastic

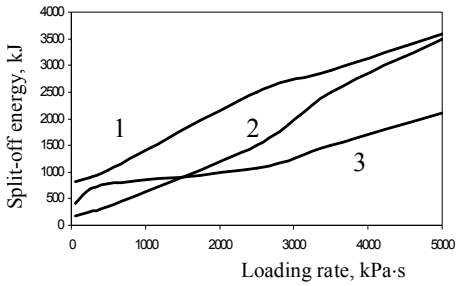

Fig. 7. The split-off energy density against the loading rate: 1—sandstone; 2—diabase; 3—marble.

modulus to drop modulus have no significant influence on the radii of the disintegration zones in rock masses.

IV. Conclusion

The authors have proposed the calculation scheme for zonal disintegration phenomenon in rocks, considering structural properties of rocks (dilatancy, internal friction angle). The conditions of a "false" contour" to generate geometric progression with denominator $\sqrt{2}$ have been determined.

References

[1] Z.T. Bieniawsky, H.G. Denkhaus, O.W. Vogler Failure of fractured rock // Int. I. Rock Mech. Sce. 1969. Vol. 6. №3.
[2] H. Bok Introduction in mechanics of rocky breeds. Under. edit. M - Mir, 1983. 276p.
[3] R. Goodman Mechanics of rocky breeds. M Stroiizdat 1987. 232p.
[4] A.M. Kovrijnyh About long durability of metals and model of ideal creep//DASc. The technical physics. M.: Science 2008. Vol. 415 №1 p. 48-51
[5] M.V. Kurlenja, V.N. Oparin About the scale factor of the phenomenon of zone disintegration of rocks and initial numbers of atomno-ionic radiuses// Fiz.-Tekh. Probl. Razrab. Polezn. Iskop. 1996. № 2.
[6] V.N. Oparin, A.P. Tapsiev, M.A. Rosenbaum, V.N. Reva, B.P. Badtiev, E.A. Tropp, A.I. Chanyshev Zonal disintegration of rocks and stability of underground excavations. Sc: the Siberian Branch of the Russian Academy of Science, 2008. 300p.
[7] A.I. Chanyshev Construction of passport dependences of rocks in prelimit and beyond the limit areas of deformation// Fiz.-Tekh. Probl. Razrab. Polezn. Iskop . 2002. № 5.
[8] A.I. Chanyshev, V.M. Zhigalkin, O.M. Usoltseva About construction of the equations of a condition of semifragile materials by data of biaxial tests// Fiz.-Tekh. Probl. Razrab. Polezn. Iskop. 2003. № 4.
[9] E.I. Shemjakin, G.L. Fisenko, M.V. Kurlenja, V.N. Oparin The effect of zonal disintegration of rocks round underground excavations //DASc USSR. 1986. V. 289. № 5.
[10] E.I. Shemjakin, M.V. Kurlenja, V.N. Oparin, V.N. Reva Rosenbaum M. A. Opening № 400 USSR. The phenomenon of zonal dicimposition of rocks round underground excavations//BI. 1992. № 3.

ISBN: 978-988-19252-2-0
ISSN: 2078-0958 (Print); ISSN: 2078-0966 (Online)